DESIGN AND DYNAMIC CHARACTERISTICS OF A LIQUID-PROPELLANT THRUST CHAMBER

Avandelino Santana Junior
Instituto de Aeronáutica e Espaço, Centro Técnico Aeroespacial, IAE/CTA,
CEP 12228-904 - São José dos Campos, SP, Brasil. E-mail: junior@mec.ita.cta.br
Luiz Carlos Sandoval Góes
Instituto Tecnológico de Aeronáutica, ITA,
CEP 12228-900 - São José dos Campos, SP, Brasil. E-mail: goes@mec.ita.cta.br

Abstract. *According to the national program for space activities (PNAE), which is elaborated by the Brazilian space agency (AEB), the liquid propulsion technology is essential in the development of the next launch vehicle, called VLS-2. The advantages of liquid-propellant rocket engines are their high performance compared to any other conventional chemical engine and their controllability in terms of thrust modulation. Undeniably, the most important component of these engines is the thrust chamber, which generates thrust by providing a volume for combustion and converting thermal energy to kinetic energy. This paper presents the design and the dynamic analysis of a thrust chamber, which can be part of the future Brazilian rocket. The basic components of the thrust chamber assembly are described, a mathematical model for simulation of the system at nominal regime of operation is constructed, and the dynamic characteristics including the stability analysis are briefly discussed.*

Keywords: *Liquid rocket engine, liquid propulsion, rocket engine design, dynamic modeling, dynamic analysis.*

1. INTRODUCTION

The design of an engine and its components is not a simple task, especially concerning liquid-propellant engine system, because it includes complex and multidisciplinary problems. Since rocket engines are airborne devices, a desirable thrust chamber combines lightweight construction with high performance, simplicity, and reliability (Sutton, 1986).

Stable operation is also a design prerequisite for rocket engine chambers, however pressure fluctuations are always present during their run. Such oscillations are caused mainly by the intrinsic combustion process, high frequency instability, and the coupling between the propellant feed system, the rocket engine and vehicle structure, low frequency instability (Huzel & Huang, 1992).

Such dynamic problems are greatly affected by design issues, for instance: dimension of injector, component configuration, and chamber length. Hence, it is important to address the question of dynamic during the engine design. Thus, in this paper, the design characteristic of a thrust chamber is described, as well as its dynamic characteristic is analyzed.

The purpose of this liquid propellant chamber, working with liquid oxygen and kerosene,

is to be part of a future Brazilian launch vehicle. All functional requirements of the engine are established beforehand to meet the mission goal and they dictate the technological concepts and the design solutions that are adopted and described in the following section.

2. DESIGN CHARACTERISTICS OF A THRUST CHAMBER

According to Sutton (1986), a thrust chamber comprises three major parts, the injector head, the combustion chamber, and the nozzle, which are shown in Fig. 1.

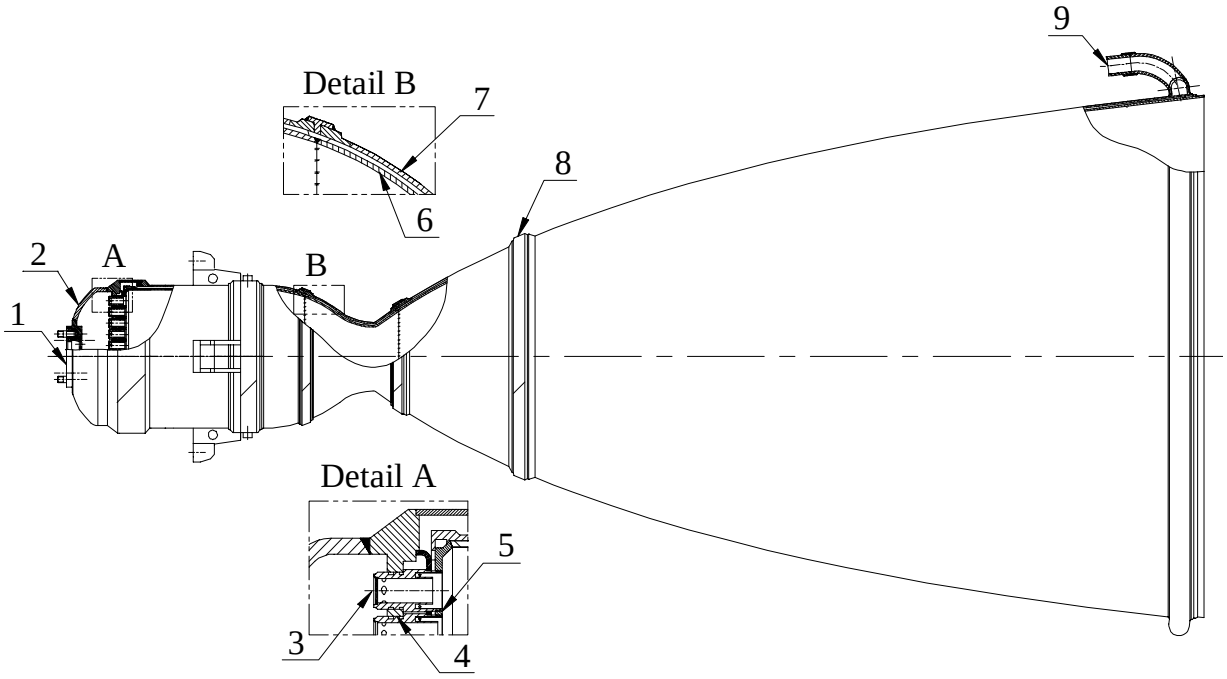

Figure 1 - Thrust chamber assembly.

2.1 Injector head design

The injector head consists of the outer bottom (2) with a flange (1), the injector (3), and the fire bottom (5). Fuel and oxidizer are kept separate by the middle bottom (4). The oxidizer cavity is located between middle bottom and outer bottom. The oxidizer is fed into cavity through the flange then it flows to tangential passages of the oxidizer injector. The fuel cavity is located between middle and fire bottoms. The fuel flows from cooling jacket to tangential passages of the fuel injector, before it cools the fire bottom.

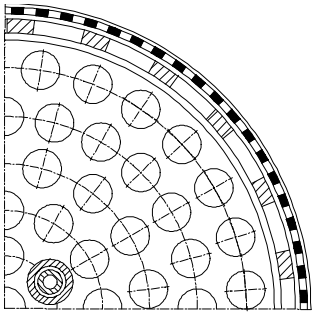

Figure 2 - Partial injector head view.

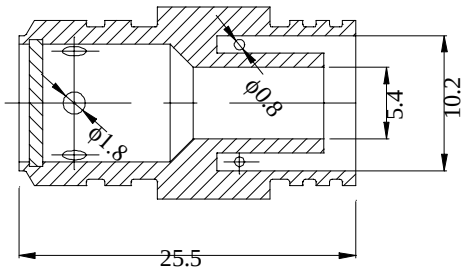

Figure 3 - Swirl injector dimensions, mm.

The final injector head configuration, including the positions of each injector, manifold, and propellant line connection is determined geometrically. Figure 2 shows part of 91 injectors installed concentrically at injector head. Each injector is a bipropellant swirl type, as it is shown in Fig. 3.

2.2 Combustion chamber design

The combustion chamber, which is shown in Fig. 1, was designed with large structural margins of safety in order to withstand all possible operating conditions. Its inner wall (6) is manufactured from a high-temperature stainless steel 1.5 mm thick. The outer shell (7) is made of a plastic stainless steel 2.25 mm thick. The distance between the walls is 2 mm, such space is called cooling jacket, and permits the flow of the fuel along the chamber, providing an efficient regenerative cooling system. The maximum fuel speed inside the cooling jacket is 22 m/s, and the total pressure drop is 1.73 MPa. Additionally, to reduce the transfer of heat in the critical region, there is a film cooling ring that allows the fuel liquid to be injected into the chamber to form a protective film of liquid adjacent to the walls. It is located at the end of the cylindrical part of the chamber, immediately upstream of the nozzle throat. The flow rate of film cooling corresponds to 1.9% of the total mass flow rate of the chamber. As result the maximum wall temperature on the gas side is 608.5 K and on the liquid side is 408.6 K, the gas temperature in the combustion chamber core is constant and equal to 3672.55 K.

2.3 Nozzle design

The nozzle in Fig. 1 is contour type, which was profiled with help of the characteristic method with free expansion of exhaust gases. This shape has better performance and is shorter than conical one. Milling ribs of the cooling jacket provide rigidity to whole wall. The fuel inlet manifold (9) is welded at the end of the nozzle for two reasons: for increasing the rigidity and for suitable distribution of regenerative cooling. Nozzle part connection is carried out by welding two halves ring (8) on the shell. The exit angle of nozzle, equal to 6º, is chosen according to optimization scheme of payload as function of mass of construction (nozzle mass) and impulse specific (Santana Jr., 1998). The nozzle contraction half angle (35.72º) is set according to gas free expansion. These angles are connected by smooth and continuous radial transitions, which allows smooth flow conditions to exist throughout the nozzle and thus minimize losses.

2.4 Thrust chamber design and performance parameters

The design and performance parameters of the thrust chamber are obtained by systematic calculation and are summarized in the Tab. 1. The geometry associated with combustion chamber and nozzle is calculated by equations derived from basic thermodynamic, pressure and force relations, the internal chamber contour is shown in the Fig. 4 (Santana Jr., 1998).

Table 1 - Thrust chamber parameters.

Run duration	150 s
Thrust level	73270 N
Vacuum specific Impulse	3589.8 m/s
Chamber pressure	8 MPa
Expansion pressure ratio	1000
Propellant mixture ratio (O/F)	2.469
Propellant mass flow rate	21.243 kg/s
Thrust chamber efficiency	0.974

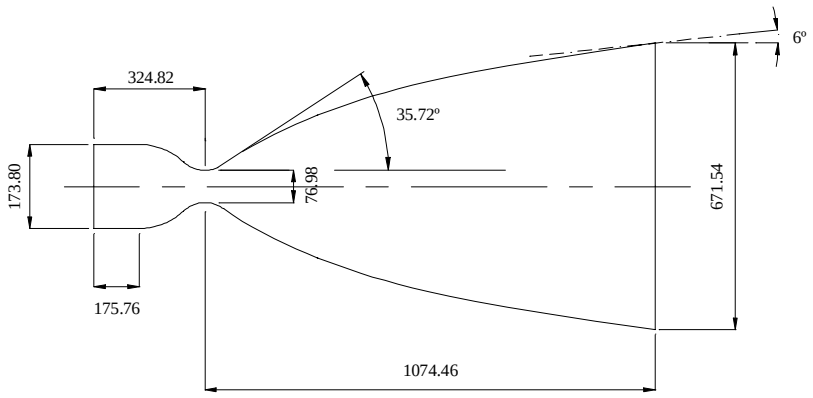

Figure 4 - Thrust chamber dimensions, mm.

Briefly discussed design solutions, as well as all parameters described here are necessary to build the mathematical model of the thrust chamber system. Such modeling permits to simulate and analyze the system stability, in this manner the purpose of the next section is to summarize various important aspects of thrust chamber dynamics.

3. DYNAMIC CHARACTERISTICS OF THE THRUST CHAMBER

The modeling of the thrust chamber, at the nominal regime of operation, is carried out by means of the knowledge of its working principle and design characteristics. The linear mathematical model of the combustion chamber, injector head and cooling jacket is obtained analytically, using the Laplace transform to change from the time domain to complex *s*-plane domain. Hereinafter for any parameter time dependent *X(t)* is expressed as follows:

$$X(t) = X + \Delta X(t), \tag{1}$$

where X is the nominal value and $\Delta X(t)$ is its pulsation component whose dimensionless form is:

$$\overline{\Delta X(t)} = \frac{\Delta X(t)}{X}. \tag{2}$$

3.1 Combustion chamber modeling

A simple analysis based on mass conservation together with some simplification leads to combustion chamber dynamic equation for the parameters at the nominal regime of operation (Santana Jr. & Góes, 1999). The transfer function relating the pressure in the combustion chamber p_c, the fuel mass flow rate $\dot{m}_f$, and the oxidizer mass flow rate $\dot{m}_o$ while considering the time delay effect τ is obtained as follows:

$$(T_c s + 1) \cdot \overline{\Delta p_c} = e^{-s\tau} \cdot \left(K_1 \cdot \overline{\Delta \dot{m}_o} + K_2 \cdot \overline{\Delta \dot{m}_f}\right). \tag{3}$$

According to Gladkova (1997), the burning process time constant T_c, the gain constants for the oxidizer line K_1 and for the fuel pipeline K_2 are respectively:

$$T_c = \frac{V \cdot C^*}{R \cdot T \cdot A_t} \cdot \phi, \tag{4}$$

$$K_1 = \frac{(O/F)}{(O/F)+1}, \text{ and} \tag{5}$$

$$K_2 = \frac{1}{(O/F)+1}. \tag{6}$$

A_t is the throat area, C^* is the gas characteristic velocity, V is the chamber volume, T is the gas temperature, R is the gas constant, (O/F) is the propellant mixture ratio, Φ is the burning and nozzle efficiency.

3.2 Injector head modeling

From dynamics standpoint, a swirl injector is a much more complicated element than a jet injector is. The main difference lies in the mechanisms of disturbance propagation between combustion chamber and the feed system (Bazarov & Yang, 1998).

For the sake of simplification, in this paper the injectors are modeled as jet one whose length is much less than the wavelength of oscillation. The linear dynamics of such short injector with passage area (A_{in}) and length (L_{in}) are obtained from flow equations using energy, momentum, and mass continuity laws (Kessaev, 1997).

It is assumed that the propellant is incompressible, the walls of the injector are rigid, and the heat transfer problem is neglected. For the liquid oxygen injectors, the transfer function relating to mass flow rate through injector head $\dot{m}_{in}$, the pressure of propellant injection p_{in} and combustion chamber p_c is:

$$\overline{\Delta\dot{m}_{in}} \cdot (T_{in}s + 1) = K_3 \cdot \overline{\Delta p_{in}} + K_4 \cdot \overline{\Delta p_c}. \tag{7}$$

The gain constants K_3 and K_4, and the time constant of liquid oxygen injectors (T_{in}) are:

$$K_3 = \frac{1}{2} N_{in} \cdot \mu_{in} \cdot A_{in} \sqrt{\frac{2\rho_{lox}}{(p_{in} - p_c)}} \cdot \frac{p_{in}}{\dot{m}_{in}}, \tag{8}$$

$$K_4 = -\frac{1}{2} N_{in} \cdot \mu_{in} \cdot A_{in} \sqrt{\frac{2\rho_{lox}}{(p_{in} - p_c)}} \cdot \frac{p_c}{\dot{m}_o}, \text{ and} \tag{9}$$

$$T_{in} = \frac{\rho_{lox} \cdot N_{in}^2 \cdot \mu_{in}^2 \cdot A_{in} \cdot L_{in}}{\dot{m}_o}, \tag{10}$$

where ρ_{lox} is the liquid oxygen specific mass, N_{in} is the number of injectors, μ_{in} is the discharge coefficient. The same procedure is applied to obtain the gain constants of the kerosene injector, K_5 and K_6, and its time constant.

3.3 Cooling jacket modeling

The flow inside the channels of the cooling jacket is assumed one-dimensional with certain fluid inertia; the friction is considered a fluid resistance and the kerosene specific mass ρ_{ker} is not constant. The discharge coefficient μ_{cj} is obtained experimentally (Kessaev, 1997). The Laplace transform for the cooling jacket taking into account the liquid compressibility and the channel elasticity is described as:

$$(I_{cj}C_{cj}s^2 + R_{cj}C_{cj}s + 1) \cdot \overline{\Delta p_{cj}} = K_7 \cdot \overline{\Delta p_i} + K_8 \cdot (T_{cj}s + 1) \cdot \overline{\Delta\dot{m}_{cj}}. \tag{11}$$

where the gain constant K_7 and K_8, and the time constant of the cooling jacket T_{cj} are, respectively:

$$K_7 = \frac{p_i}{p_{in}}, \tag{12}$$

$$K_8 = -\frac{\dot{m}_{cj}^{\,2}}{p_{in} \cdot \rho_{ker} \cdot \left(\mu_{cj} A_{cj}\right)^2}, \text{ and} \tag{13}$$

$$T_{cj} = -\frac{L_{cj} \cdot \dot{m}_{cj}}{A_{cj} \cdot p_{cj}} \cdot \frac{1}{K_8}. \tag{14}$$

Considering the cooling jacket as a tube with equivalent length L_{cj}: p_i represents the pressure at fuel inlet manifold, $\dot{m}_{cj}$ is the mass flow rate, A_{cj} is the cross-sectional area. The fluid inertia in the cooling jacket I_{cj}, the equivalent capacitance C_{cj} and the liquid resistance R_{cj} are described as:

$$I_{cj} = \frac{L_{cj} \rho_{ker}}{A_{cj}}, \tag{15}$$

$$C_{cj} = \frac{V_{cj}}{\beta_{ker}} + V_{cj} \cdot \frac{2r_{cj}}{Et_{cj}}, \text{ and} \tag{16}$$

$$R_{cj} = \frac{\dot{m}_i}{\left(\mu_{cj} A_{cj}\right)^2}, \tag{17}$$

where E is the elastic modulus of the tube, $\dot{m}_i$ is mass flow rate at fuel inlet manifold, t_{cj} is the thickness of the wall channel, r_{cj} is the internal radius of equivalent tube, V_{cj} is the liquid volume, and β_{ker} is kerosene *Bulk modulus*.

Connecting all components and defining numerically the time constants and gains of the mathematical model allows the construction of the block diagram, as it is shown in Fig. 5, which can be used to simulate and to analyze the system stability.

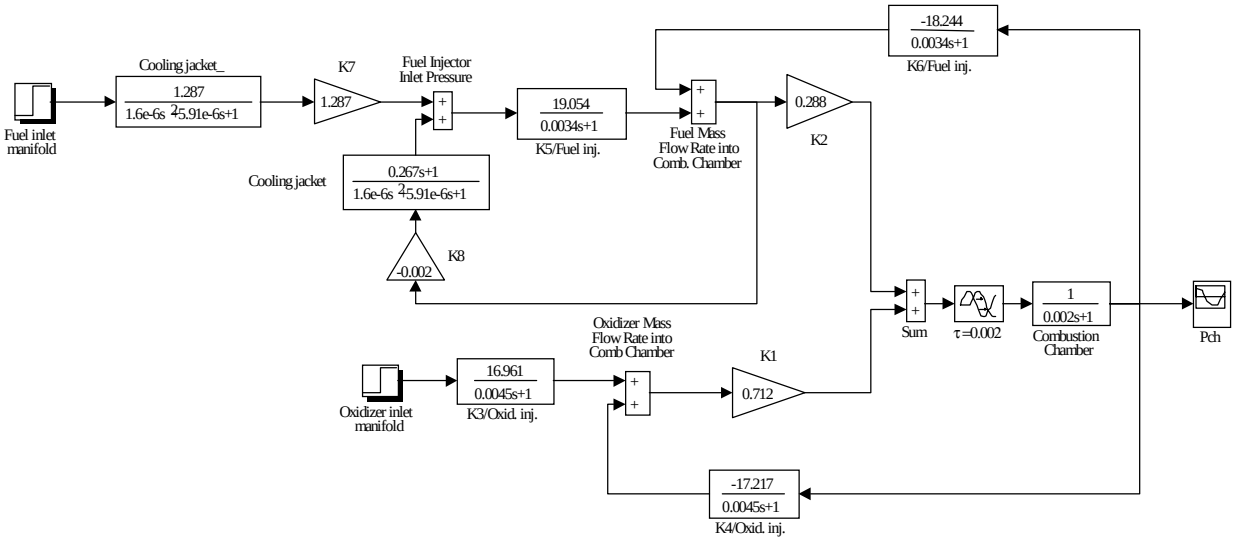

Figure 5 - Thrust chamber block diagram representation.

3.4 Trust chamber frequency response

The frequency response of a system is defined as the steady-state response of the system to a sinusoidal input signal. The assessment of the stability performance in the frequency domain can be carried out by means of two different diagrams, Nyquist and Bode plots.

Figure 6 shows that the system is stable by the Nyquist criterion of stability. The concept of relative stability can be established by the gain margin (GM) and phase margin (PM) for a rated range of frequency in the Bode plot, as it is presented in Fig. 7.

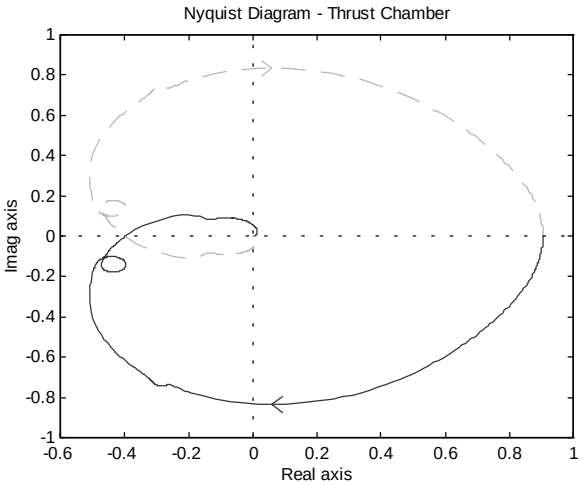

Figure 6 - Nyquist plot, frequency runs changes from -∞ to +∞.

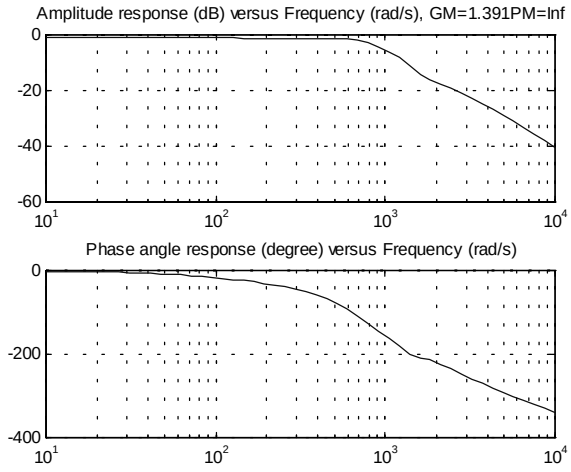

Figure 7 - Bode plot, frequency runs from 1.5 Hz to 1500 Hz.

3.5 Thrust chamber stability analysis

Several techniques have been developed for stability analysis, which can be used for two purposes, to know if the system is stable or not and to obtain a region of stability. Recently, two different methods were applied to construct such region, Mikhailov and Hermite-Biehler criteria, for three parameters that have great influence on frequency oscillations development of combustion chambers (Santana Jr. & Góes, 1999).

In this manner, the Routh-Hurwitz criterion also can be applied to find the zones of stability for the same analyzed parameters (Fig. 8). However, the time constant of combustion chamber T_c and the time delay of the combustion process τ constitute another plane.

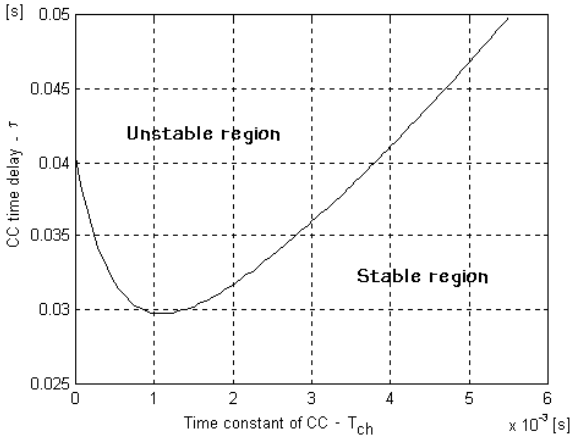

Figure 8 - Zone of stability in the plane time constant - time delay by Routh criterion.

The procedure involves selecting a range of values for these two parameters, computing the roots of the characteristic equation (Eq. 18) for specific values of them. For each value of T_c is found the first value of τ that result in at least one root of the characteristic equation in the half-right plane. This process is repeated until the entire selected range of T_c and τ is exhausted. Then, the plot of these pairs defines the separation between the stable and unstable regions.

$$\begin{aligned}\delta(s) = {} & 0.00111859 \cdot T_c \tau\, s^4 + (0.00223718 \cdot T_c + 0.00111859 \cdot \tau + 1.39412 \cdot T_c \tau) s^3 + \\ & + (0.00223718 + 2.78824 T_c + 0.274792 \tau + 204.62 T_c \tau) s^2 + \\ & + (5.02689 + 409.24 T_c - 47.7664 \tau) s + 914.013\end{aligned} \tag{18}$$

The designed system parameters, T_c =0.002 s and τ =0.002 s, are inside the stable region.

4. CONCLUSION

From the previous summary about the design of a liquid oxygen/kerosene thrust chamber, it can be concluded that such preliminary design meet the requirements of the technical specification for a second stage rocket engine. Because of high combustion temperature and high heat transfer rates from the hot gases to the chamber wall, two cooling techniques were used: regenerative and film cooling.

The dynamic analysis deserves special consideration during engine design, because potential mechanisms of chamber pressure oscillations can generate instability problems. Thus, the modeling of the combustion chamber, injector head, and cooling jacket was carried out. The Bode and Nyquist diagrams showed that the system is stable. In addition, the region of stability was obtained, for the two parameters, τ and T_c, by means of Routh-Hurwitz criterion, and for their nominal values, the system is stable.

5. REFERENCES

BAZAROV, V. G. and YANG, V., 1998, "Liquid-Propellant Rocket Engine Injector Dynamics". Journal of Propulsion and Power, v.14.

GLADKOVA, V. N., 1997, "Theory of Rocket Engines Automatic Control Systems". In: Fundamental Course in Engine Design. São José dos Campos, CTA/IAE.

HUZEL, D. K. and HUANG, D. H., 1992, "Modern Engineering for Design of Liquid-Propellant Rocket Engines". Washington: AIAA.

KESSAEV, J., 1997, "Theory and Calculation of Liquid-Propellant Engine". In: Fundamental Course in Engine Design. São José dos Campos: CTA/IAE.

SANTANA JR., A., 1998, "Diploma Project: Design of a Liquid Rocket Engine". In: Fundamental Course in Engine Design. São José dos Campos: CTA/IAE.

SANTANA JR., A. and GÓES, L.C.S., 1999, "Dynamic Modeling and Stability Analysis of a Liquid Rocket Engine". 15th Brazilian Congress of Mechanical Engineering, COBEM, Águas de Lindóia/SP.

SUTTON, G. P., 1986, "An Introduction to Rocket Propulsion". New York: John Wiley & Sons.